ACS OMEGA

http://pubs.acs.org/journal/acsodf

Article

Role of NOM in the Photolysis of Chlorine and the Formation of Reactive Species in the Solar/Chlorine System

Huaxi Zhou and Dongxue Xiao*

Cite This: *ACS Omega* 2022, 7, 7769−7776

Read Online

ACCESS | Metrics & More | Article Recommendations | Supporting Information

ABSTRACT: The solar/chlorine system has been proposed as a novel advanced oxidation process (AOP) for efficient pollutant degradation and water disinfection by producing a series of reactive species including hydroxyl radicals (HO•), chlorine radicals (Cl•), and so forth. In this study, the role of natural organic matter (NOM) in the photolysis of free available chlorine (FAC) and the formation of HO• and Cl• in the solar/chlorine system was investigated employing nitrobenzene and benzoic acid as selective chemical probes. The decay rate of FAC was significantly accelerated in the presence of NOM at pH 5.5 under simulated solar irradiation, likely due to the photoreaction between FAC and the photoexcited NOM. The decay rate of FAC increased upon increasing the electron-donating capacity of NOM, which indicated that phenolic components play a significant role in the photodegradation of FAC. This acceleration mechanism was further verified using 4-nitrophenol as a model phenolic compound. NOM promoted Cl• formation and quenched HO• in the solar/chlorine system. The proposed reaction mechanism included the reaction of excited singlet phenolic compounds in NOM with FAC, which yielded Cl•. This study provides a useful insight into future applications for using the solar/chlorine system as a novel AOP for wastewater treatment or disinfection.

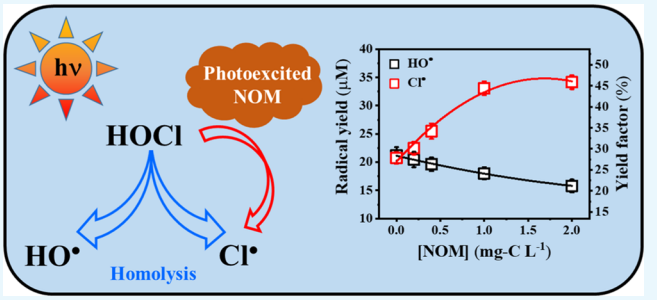

INTRODUCTION

Chlorine is used worldwide to disinfect drinking water and recreational water.[1,2] The combination of chlorine with UV-C light (UV/chlorine system) is an advanced oxidation process (AOP) that is highly efficient for degrading organic contaminants in industrial and domestic wastewater by producing reactive species (RS) such as HO•, reactive chlorine species, and so forth.[3−9] The main drawback of the UV/chlorine system is the high operating costs of UV lamps; thus, employing sunlight as an alternative driving force to initiate chlorine (solar/chlorine system) has received increasing attention due to the overlap in the absorption spectrum of chlorine and the solar spectrum.[10−20]

The solar/chlorine system relies on the photolysis of aqueous free available chlorine (FAC), which consists of HOCl (pK_a = 7.5 at 25 °C) and its conjugate base ClO^- at environmentally relevant pH values. Previous studies have shown that a series of RS are generated during the photolysis of FAC under solar irradiation.[21−23]

$$HOCl + h\nu \rightarrow HO^\bullet + Cl^\bullet \quad (1)$$

$$ClO^- + h\nu \rightarrow O^{\bullet -} + Cl^\bullet \quad (2)$$

$$ClO^- + h\nu \rightarrow O(^3P) + Cl^- \quad (3)$$

$$O(^3P) + O_2 \rightarrow O_3 \quad (4)$$

$$HO^\bullet/Cl^\bullet + HOCl \rightarrow ClO^\bullet + H_2O/HCl \quad (5)$$

$$HO^\bullet/Cl^\bullet + ClO^- \rightarrow ClO^\bullet + HO^-/Cl^- \quad (6)$$

$$Cl^\bullet + Cl^- \rightarrow Cl_2^{\bullet -} \quad (7)$$

As shown in eqs 1−3, RS, including HO•, the conjugate base of HO• ($O^{\bullet -}$), Cl•, and $O(^3P)$ are generated from the direct photolysis of FAC. $O(^3P)$ can further react with molecular oxygen to yield O_3 via eq 4. In addition, secondary chlorinated radicals ClO• and $Cl_2^{\bullet -}$ are generated via reactions of HO•/Cl• with FAC and Cl• with chloride, respectively, as presented in eqs 5−7. HO• and Cl• are powerful oxidizing species that can react with most organic compounds through hydrogen abstraction or addition reactions at almost diffusion-controlled rates, while O_3, ClO•, and $Cl_2^{\bullet -}$ have narrower reactivity spectra than HO• and Cl• (but still broad) due to their lower one-electron reduction potentials than HO• and Cl•.[24−26]

The solar/chlorine system can disinfect and degrade pharmaceuticals and personal care products (PPCPs) in

Received: November 23, 2021
Accepted: February 14, 2022
Published: February 23, 2022

https://doi.org/10.1021/acsomega.1c06616
ACS Omega 2022, 7, 7769−7776

water. For example, a dramatically enhanced inactivation of *Bacillus subtilis* spores and *Cryptosporidium parvum* oocysts was observed when they were treated by the solar/chlorine system compared with chlorination or sunlight alone.[11,13] $HO^{\bullet}$ and O_3 played a critical role in pathogen inactivation. Furthermore, the solar/chlorine system was also used for the remediation of oil sand process-affected water (OSPW).[12] After solar/chlorine treatment, the acute toxicity of OSPW toward *Vibrio fischeri* was reduced. Similar detoxification was observed in solar/chlorine-treated herbicides by Kong and co-workers.[27] Recently, the solar/chlorine system was employed for the abatement of PPCPs in simulated drinking water and real river waters.[18,19] The pH-dependent removal of PPCPs and increasing formation of chlorinated disinfection byproducts (DBPs) were discovered during FAC photolysis under simulated solar irradiation. Great efforts have also been devoted to exploring the influence of pH and irradiation wavelength on RS formation during the photolysis of chlorine by Remucal and co-workers.[17] Under natural organic matter (NOM)-free conditions, the highest concentrations of $HO^{\bullet}$ and $Cl^{\bullet}$ were observed under acidic conditions when irradiated with lower wavelengths (254 and 311 nm), while the maximum cumulative concentrations of O_3 were observed at a higher wavelength (365 nm) under alkaline conditions.

In the solar/chlorine system, NOM generally serves as the principal sink for the added oxidant and generated RS.[18] NOM is a heterogeneous mixture of organic compounds and is ubiquitous in terrestrial and aquatic systems.[28−30] The chemical composition and physicochemical properties of NOM vary depending upon its origin (terrestrial or autochthonous).[31−33] When exposed to sunlight, ground-state NOM is excited to an excited singlet state (^{1}NOM*) that undergoes intersystem crossing and generates an excited triplet state (^{3}NOM*).[34] Excited states of NOM are both better oxidants and reductants than their ground states.[35−37] Consequently, NOM containing electron-accepting (e.g., quinones, aromatic ketones, and so forth) and electron-donating (e.g., phenols, amines, olefins, anilines, and so forth) functional groups are susceptible to chemical modifications during the exposure of NOM to FAC and RS generated in the solar/chlorine system. Additionally, NOM is the most important DBP precursor during the chlorination of drinking water.[16,19,38,39]

In this study, the decay of FAC was investigated under simulated solar irradiation at pH 5.5 because the solar/chlorine system exhibited more efficient pollutant degradation and water disinfection under acidic conditions than under neutral or alkaline conditions.[14,17] The role of NOM on the FAC decay rate was also studied with different NOM concentrations. Dissolved oxygen (DO) control experiments, electron-donating capacity (EDC) measurements, and a model phenolic compound (4-nitrophenol) were employed to elucidate the role of photoexcited NOM in the acceleration of FAC photolysis under simulated solar irradiation. Mathematical models were established to quantitatively determine the formation of $HO^{\bullet}$ and $Cl^{\bullet}$ in the solar/chlorine system using nitrobenzene (NB) and benzoic acid (BA) as selective chemical probes. The effect of NOM on the formation of $HO^{\bullet}$ and $Cl^{\bullet}$ was examined, and the reaction mechanism between FAC and the excited singlet phenolic compound in NOM was proposed.

EXPERIMENTAL SECTION

Chemicals. Suwannee River NOM (SRNOM, no. 2R101N), Suwannee River fulvic acid (SRFA, no. 2S101F), Pony Lake fulvic acid (PLFA, no. 1R109F), and Waskish Peat fulvic acid (WPFA, no. 1R107F) were obtained from the International Humic Substances Society. Effluent organic matter (EfOM) was isolated from the secondary effluent collected from the Quyang municipal sewage plant in Shanghai, China. The isolation method previously reported by Bodhipaksha et al. was used with slight modifications and provided in Text S1 of the Supporting Information (SI).[40,41] NB (99%), BA (99%), trifluoroacetic acid (TFA, 99%), sodium hypochlorite (NaClO, 4.00−4.99%), 4-nitrophenol (99%), sodium tetraborate decahydrate ($Na_2B_4O_7{\bullet}10H_2O$, 99%), and phosphate salts (NaH_2PO_4 and Na_2HPO_4, both 99%) were purchased from Sigma-Aldrich. 2,2′-Azino-bis (3-ethylbenzothiazoline-6-sulfonic acid diammonium salt) (ABTS, 98%) was purchased from Tokyo Chemical Industry Co., Ltd. *N*,*N*-Diethyl-*p*-phenylenediamine (DPD) free-chlorine reagent was provided by HACH Co., Ltd. All chemicals were used as received except for sodium hypochlorite, which was standardized using a UV−vis spectrometer (ε_{292} = 365 M^{-1} cm^{-1}). The FAC content was measured using the DPD colorimetric method.[42]

Photochemical Experiments. Reaction solutions were illuminated in a solar simulator (Suntest XLS$^+$ Atlas) equipped with a 1700 W xenon lamp. A solar filter was employed to block irradiance below 290 nm. The chamber temperature was maintained at 25.0 ± 1.0 °C using a temperature control unit (Suncool). The fluence rate at the surface of the solutions was set to 40 W m^{-2} (1.36 × 10^{-8} E s^{-1} cm^{-2}) at 290−400 nm. The absolute irradiance spectra of the simulated solar light and real sunlight were recorded using a spectra-radiometer (USB-4000, Ocean Optics, Inc.) and are presented in Figure S1 of the Supporting Information. Samples (20.0 mL) buffered at pH 5.5 by 10.0 mM phosphate buffer were placed in specially made cylindrical quartz containers (diameter = 6.0 cm, height = 2.0 cm, thickness = 0.2 cm, as described in our previous study[43]) and irradiated for 1 h under ambient conditions for radical yield experiments. The FAC dosage in the solution was 53.7 μM (note: no FAC was detected after 1 h of irradiation). After illumination, aliquots were removed and analyzed by HPLC−UV (Agilent 1260). For FAC decay experiments, 100.0 mL of the samples was irradiated for 5 min. After illumination, aliquots were removed and analyzed using the DPD colorimetric method. The dissolved organic carbon was measured using a TOC analyzer (Sievers M9, USA). The concentration of DO was measured using a DO meter (WTW, Germany). For the oxygen-dependent experiments, high-purity nitrogen, oxygen, or mixtures were slowly purged into the reaction vessel (the flow rate was approximately 150 mL min^{-1}). Otherwise, the DO concentrations in the reaction solutions were kept nearly constant (about 250 μM) during 1 h of irradiation under air-saturated conditions. UV−vis absorbance spectra of FAC (1.34 mM) at pH 5.5 were collected in a 1 cm quartz cuvette using a spectrophotometer (Cary 60, Agilent) and are shown in Figure S1 of the Supporting Information. All solutions were prepared in deionized (DI) water (18.25 MΩ). The error bars in the corresponding figures represent the standard deviation of three replicates.

https://doi.org/10.1021/acsomega.1c06616
ACS Omega 2022, 7, 7769−7776

Analytical Methods. NB (5−100 μM) and BA (5−200 μM) were analyzed using an high-performance liquid chromatograph (Agilent 1260 system) equipped with a photodiode array detector and a C_{18} column (4.6 × 250 mm, 5 μm, Phenomenex Luna). All separations were achieved with an isocratic mobile phase consisting of methanol (MeOH) and water acidified with TFA (0.05%) at a flow rate of 1.0 mL min^{-1}. The volumetric ratio of MeOH/acidified water was 50:50, and the column temperature was 30 °C for both probes. The detection wavelength was 266 nm for NB and 240 nm for BA.

EDC Quantification. The previously developed liquid system for quantifying the EDC values in organic matter is provided in Scheme S1 of the Supporting Information and briefly discussed below.[44] The carrier solution A (50.0 mM borate at pH 7.8) was continuously delivered through a quaternary pump (Agilent HPLC 1260) at a flow rate of 0.2 mL min^{-1}. The organic matter samples (100 μL, 5.0 mg-C L^{-1}) were injected using an LC auto-sampler (Agilent HPLC 1260). Solution B (containing 0.1 mM ABTS$^{\bullet+}$, 10.0 mM H_2SO_4, and 7.0 mM chlorine at pH 4.6) was continuously delivered through a binary pump (Agilent HPLC 1290) at a flow rate of 0.08 mL min^{-1}. The two solutions were then passed through a reaction coil (0.254 mm, 20 m) to ensure the full oxidation of EDC by ABTS$^{\bullet+}$. By monitoring the integrated area of the absorbance peak at 405 nm (characteristic absorption of ABTS$^{\bullet+}$), the EDC values were calculated using eq 8

$$\mathrm{EDC} = -\frac{1}{m_C}\left(q_V \frac{\int (A_{405}(t) - A_{405,\mathrm{baseline}})\mathrm{d}t}{\varepsilon_{405} \bullet l}\right) \quad (8)$$

where m_c represents the mass of the injected carbon (mg-C), q_V represents the total volumetric flow rate (mL min^{-1}), ε_{405} represents the molar absorption coefficient of ABTS$^{\bullet+}$ (31,600 M^{-1} cm^{-1}), and l is the optical path length (1 cm).

RESULTS AND DISCUSSION

Photolysis of FAC. The decomposition of FAC was investigated in 10.0 mM phosphate-buffered solution at pH 5.5 under simulated solar irradiation. Under our experimental conditions, FAC decayed rapidly when exposed to sunlight; therefore, only the initial photolysis process followed pseudo-first-order kinetics and was thus employed to investigate the photolysis of FAC. Figure 1a shows a comparison of the decay of FAC under dark conditions in the NOM solution, exposure to simulated sunlight in DI water, and exposure to simulated sunlight in the NOM solution, where the same initial concentration of $[FAC]_0$ = 53.7 μM (4 mg L^{-1}) was used. FAC decomposed slowly in the NOM solution under dark conditions with a decay rate constant of 0.0036 min^{-1}. Upon solar irradiation, FAC decayed rapidly in DI water with a decay rate constant of 0.0167 min^{-1}. Similar to a previous study by Sun and co-workers,[14] a comparable decay rate constant of FAC in 10 mM PBS was obtained from the photolysis experiment under simulated solar irradiation at acidic pH (5−6), but they used a higher initial FAC concentration (7 mg L^{-1}) and stronger solar intensity. A reasonable explanation was that we only investigated the initial photolysis process, during which FAC decayed faster than in the subsequent photolysis process. In the 1.0 mg-C L^{-1} SRNOM solution, the FAC decay rate was significantly accelerated, with a decay rate constant of

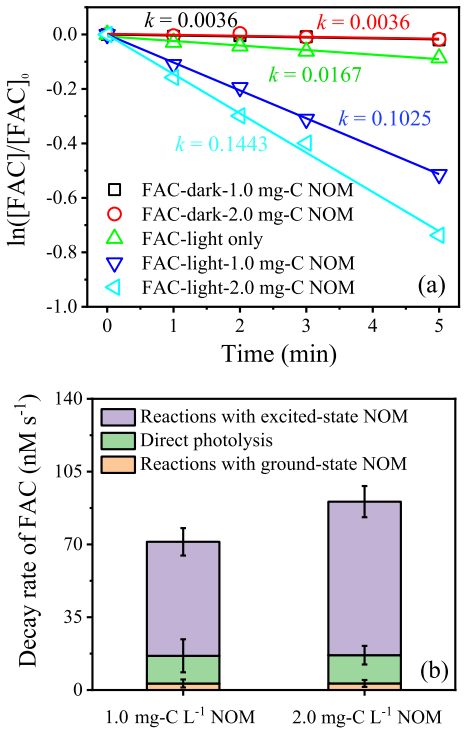

Figure 1. (a) Photolysis of FAC vs reaction time and the (b) contribution of specific pathways to the decay rate of FAC in the solar/chlorine system. Experimental conditions: FAC concentration of 53.7 μM, air saturation, 10.0 mM phosphate buffer pH 5.5, irradiation wavelength of λ > 290 nm, irradiation time 5.0 min, and NOM concentration of 1.0 or 2.0 mg-C L^{-1} (SRNOM, no. 2R101N). The error bars represent the standard deviation of three replicates.

0.1025 min^{-1}, which was approximately sixfold higher than that observed in DI water. Upon continuing to increase the SRNOM concentration to 2.0 mg-C L^{-1}, a greater FAC decay rate constant of 0.1443 min^{-1} was obtained, indicating a synergistic effect between NOM and solar light; therefore, a photoreaction must occur between FAC and NOM in the solar/chlorine system. Two possible scenarios existed in the photoreaction between FAC and NOM: (i) the excited-state FAC reacted with the ground-state NOM and promoted the FAC photolysis rate and (ii) the ground-state FAC reacted with the excited-state NOM and accelerated FAC photolysis.

NOM is a heterogeneous mixture that can generate a series of reactive intermediates including ^{1}NOM*, ^{3}NOM*, and charge-separated species (NOM$^{\pm}$) in sunlit surface waters. These reactive intermediates can also react with DO and produce a variety of ROS such as HO$^{\bullet}$, $^1O_2$, $O_2^{\bullet-}$, and so forth. Therefore, the latter scenario is plausible, and the specific pathway that contributed to FAC photolysis including reactions with ground-state NOM, direct photolysis, and reactions with excited-state NOM was calculated, as shown in Figure 1b. Even though excited-state NOM played a crucial role in the photolysis of FAC in the solar/chlorine system, the underlying reaction mechanism is still ambiguous.

Mechanism Elucidation. NOM was found to have dual roles in the photo-transformation of organic contaminants in surface waters.[45−48] Electron acceptors, including aromatic ketones and quinone moieties, are major contributors to photoinduced ^{1}NOM* and ^{3}NOM*, while electron donors, that is, mostly amine and phenolic constituents in NOM, show quenching effects. To examine the role of NOM during the

https://doi.org/10.1021/acsomega.1c06616
ACS Omega 2022, 7, 7769−7776

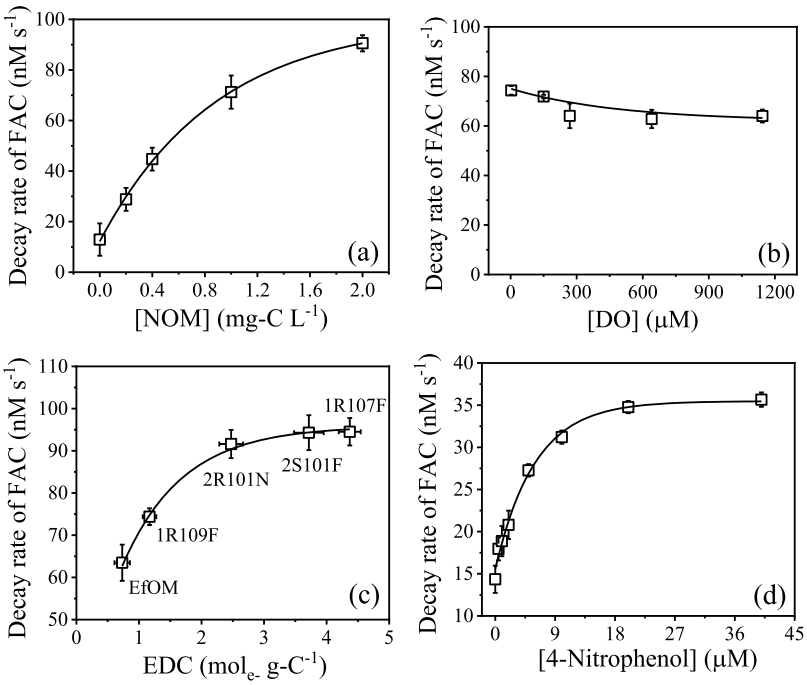

Figure 2. Decay rate of FAC vs (a) NOM concentration, (b) DO concentration, (c) EDC of organic matter, and (d) 4-nitrophenol concentration in the solar/chlorine system. Experimental conditions: FAC concentration of 53.7 μM, air saturation, 10.0 mM, phosphate buffer pH 5.5, irradiation wavelength of $\lambda > 290$ nm, and irradiation time of 5.0 min, (a) NOM concentration of 0, 0.2, 0.4, 1.0, and 2.0 mg-C L^{-1} (SRNOM, no. 2R101N), (b) NOM concentration of 2.0 mg-C L^{-1} (SRNOM, no. 2R101N), DO concentration of 3.1, 150.4, 268.8, 640.6, and 1143.8 μM, (c) organic matter concentration of 2.0 mg-C L^{-1} (including reference NOMs and EfOM), and (d) 4-nitrophenol was spiked at eight different concentrations of 0, 0.5, 1.0, 2.0, 5.0, 10.0, 20.0, and 40.0 μM. The error bars represent the standard deviations of three replicates.

photolysis of FAC in the solar/chlorine system, the relationship between the FAC decay rate and NOM concentration was studied. As shown in Figure 2a, the decay rate of FAC increased upon increasing the NOM concentration in the range of 0−2.0 mg-C L^{-1} (it should be noted that low concentrations of NOM were used in the photochemical experiments to avoid the light screening effect) under simulated solar irradiation, which further indicated that a reaction occurred between FAC and the reactive intermediate from photoexcited NOM. As mentioned above, reactive intermediates including ^{1}NOM*, ^{3}NOM*, NOM$^{\pm}$, and ROS were generated in an air-saturated NOM solution under solar irradiation. ^{3}NOM* and NOM$^{\pm}$ can react with oxygen to produce $^1O_2$ and $O_2^{\bullet-}$, respectively.[35,49,50] The disproportionation reaction of $O_2^{\bullet-}$ accounted for the main degradation pathway with a reported rate constant of 4.0×10^4 M^{-1} s^{-1},[51] which simultaneously produced H_2O_2. Fenton's reaction, one of the formation pathways of $HO^{\bullet}$, can cause the decay of H_2O_2 when a trace amount of ferrous ion is present.[52] Therefore, the concentrations of ^{3}NOM*, NOM$^{\pm}$, and ROS were highly related to the DO concentration in the solution except for ^{1}NOM*. To distinguish which reactive intermediate played a major role in accelerating FAC photolysis, the decay rate of FAC against the DO concentration was determined under simulated solar irradiation. As shown in Figure 2b, a DO concentration in the range of 3.2−1143.7 μM had a negligible influence on the decay rate of FAC, which indicated that ^{1}NOM* seemed to be the most plausible reactive intermediate responsible for accelerating the FAC decay rate in the solar/chlorine system.

The EDC value has been widely employed to investigate the redox properties of NOM (i.e., antioxidant).[40,53−55] To elucidate the reaction mechanism between FAC and ^{1}NOM* in the solar/chlorine system, the EDC values from various organic matters including the reference NOMs and EfOM were measured using a previously developed method with a liquid system as presented in Scheme S1 of the Supporting Information.[44] The EDC values calculated based on eq 8 are shown in Table S1 of the Supporting Information. In accordance with previous studies,[44] terrestrial-origin WPFA (4.37 $mmol_{e^-}$ g-C^{-1}), SRFA (3.72 $mmol_{e^-}$ g-C^{-1}), and SRNOM (2.47 $mmol_{e^-}$ g-C^{-1}) have higher EDC values than EfOM (0.73 $mmol_{e^-}$ g-C^{-1}) and autochthonous-origin PLFA (1.13 $mmol_{e^-}$ g-C^{-1}). The autochthonous-origin PLFA and EfOM had similar EDC values, suggesting that they might possess similar redox properties during photochemical reactions under identical reaction conditions.[41,56−58] The relationship between the FAC decay rate and EDC values in the solar/chlorine system was investigated. As shown in Figure 2c, the FAC decay rate increased upon increasing EDC values and followed an exponential relationship. Higher FAC decay rates were discovered in terrestrial-origin NOMs due to their higher EDC values compared with those of autochthonous-origin PLFA and EfOM. This suggests that the electron-donating components in organic matter played a vital role in promoting the FAC photolysis rate. Phenol and its derivatives were widely used as model electron-donating components in environmental photochemistry.[35,59] To further explore the mechanism for the reaction between ^{1}NOM* and FAC, 4-nitrophenol was employed to mimic the electron-donating components in NOM macromolecules. 4-Nitrophenol is an ideal model compound because the electron-withdrawing nitro group can decrease the reactivity of phenol, which prevented the direct reaction of 4-nitrophenol with FAC under dark

https://doi.org/10.1021/acsomega.1c06616
ACS Omega 2022, 7, 7769−7776

conditions. As shown in Figure 2d, an exponential relationship between the FAC decay rate and 4-nitrophenol concentration was also observed, which indicated that excited singlet phenolic compounds in NOM might play a key role in promoting the FAC decay rate in the solar/chlorine system.

Yields of HO• and Cl• in the Solar/Chlorine System. To better understand the solar/chlorine system, it is critical to quantify the effect of NOM on radical production. Since FAC decays rapidly under our reaction conditions, radical yields were investigated instead of their steady-state concentrations. Based on the Beer−Lambert law and pK_a value of HOCl (7.5 at 25 °C), HOCl (approximately 99%) was predominant in the FAC solution at pH 5.5. Consequently, two reactive radicals (HO• and Cl•) were generated from the photolysis of FAC under simulated solar irradiation at pH 5.5 via eq 1. Chemical probes NB and BA were employed together to measure the yields of HO• and Cl• in the solar/chlorine system. Cl• only reacted with BA, and HO• reacted with both probes. In the presence of NB, the formation of HO• was the sum of the consumption of the probe NB and solution scavengers (mainly FAC and NOM). In the presence of BA, both BA and solution scavengers contributed to the decay of HO• and Cl•. Thus, mathematical models were established to study the decomposition of the chemical probes NB and BA as presented in eqs 9 and 10, respectively

$$\Delta NB = F_{HO^\bullet} \times \frac{k_{HO^\bullet,\,NB}[NB]}{k_{HO^\bullet,\,NB}[NB] + k_{HO^\bullet,\,S}} \quad (9)$$

$$\Delta BA = F_{HO^\bullet} \times \frac{k_{HO^\bullet,\,BA}[BA]}{k_{HO^\bullet,\,BA}[BA] + k_{HO^\bullet,\,S}} + F_{Cl^\bullet} \times \frac{k_{Cl^\bullet,\,BA}[BA]}{k_{Cl^\bullet,\,BA}[BA] + k_{Cl^\bullet,\,S}} \quad (10)$$

where ΔNB (mol) and ΔBA (mol) represent the degradation of NB and BA, respectively; $F_{HO•}$ (mol) and $F_{Cl•}$ (mol) represent the formation of HO• and Cl•, respectively; (note: to facilitate the calculation of the radical yield, both sides of the equation were multiplied by the reaction time); $k_{HO•,NB}$ (M^{-1} s^{-1}) and $k_{HO•,BA}$ (M^{-1} s^{-1}) are the second-order rate constants for the reactions of HO• with NB and HO• with BA, respectively; $k_{Cl•,BA}$ (M^{-1} s^{-1}) is the second-order rate constant for the reaction between Cl• and BA; $k_{HO•,S}$ (s^{-1}) and $k_{Cl•,S}$ (s^{-1}) are the pseudo-first-order rate constants for solution scavengers. Previously reported second-order rate constants were employed and are shown in Table S2 of the Supporting Information.[60,61] It should be noted that the degradation of NB and BA under chlorination in the dark and under direct solar photolysis was negligible under our reaction conditions.

Different concentrations of NB and BA were employed to trap HO• and Cl• during the photolysis of FAC in DI water or NOM solutions at pH 5.5 under simulated solar irradiation. As shown in Figure 3a, the decays in NB versus NOM concentration followed exponential trends, which were fitted in Matlab with eq 9, and the formation of HO• was calculated. Meanwhile, the decays of BA versus the NOM concentration were fitted in Matlab employing eq 10, as displayed in Figure 3b. With the known value of the formation of HO• obtained from Figure 3a, the formation of Cl• was then calculated.

The yields of HO• and Cl• in the solar/chlorine system are shown in Figure 4. The yield of HO• from the photolysis of FAC in DI water was 21.2 μM with a yield factor (radical yield/$[FAC]_0$) of 28.4%, which was slightly higher than the yield of Cl• (20.7 μM) with a yield factor of 27.8%. Under our reaction conditions, HO• and Cl• were quenched by HOCl

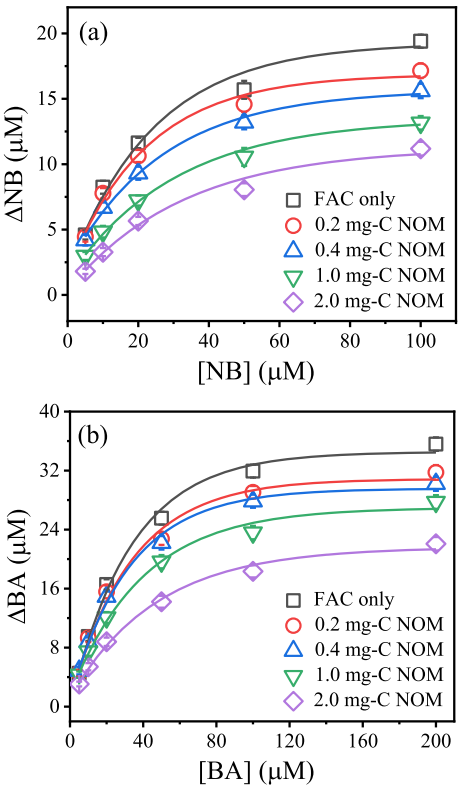

Figure 3. Photodegradation as a function of the probe concentration in the solar/chlorine system for (a) NB and (b) BA. Experimental conditions: NB and BA were spiked at different concentrations of 5.0, 10.0, 20.0, 50.0, and 100.0 μM for NB and 5.0, 10.0, 20.0, 50.0, 100.0, and 200 μM for BA, FAC concentration of 53.7 μM, NOM concentration of 0, 0.2, 0.4, 1.0, and 2.0 mg-C L^{-1} (SRNOM, no. 2R101N), air saturation, 10.0 mM phosphate buffer pH 5.5, irradiation wavelength of λ > 290 nm, and irradiation time of 1.0 h. The error bars represent the standard deviation of three replicates.

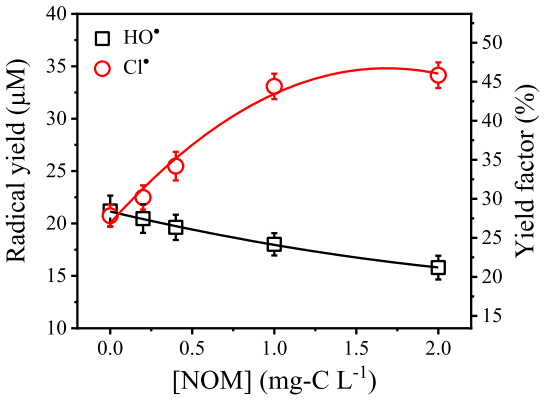

Figure 4. Influence of NOM concentration on the yields of HO• and Cl• in the solar/chlorine system. Experimental conditions: NB and BA were spiked at different concentrations with 5.0, 10.0, 20.0, 50.0, and 100.0 μM for NB and 5.0, 10.0, 20.0, 50.0, 100.0, and 200 μM for BA, FAC concentration of 53.7 μM, NOM concentration of 0, 0.2, 0.4, 1.0, and 2.0 mg-C L^{-1} (SRNOM, no. 2R101N), air saturation, 10.0 mM phosphate buffer pH 5.5, irradiation wavelength of λ > 290 nm, and irradiation time of 1.0 h. The error bars represent the standard deviation of three replicates.

https://doi.org/10.1021/acsomega.1c06616
ACS Omega 2022, 7, 7769−7776

and yielded $ClO^{\bullet}$ via eq 5, which resulted in low yield factors for $HO^{\bullet}$ and $Cl^{\bullet}$. Approximately equal values were observed in the yield of $HO^{\bullet}$ and $Cl^{\bullet}$, which indicated that the photolysis of FAC proceeded through a homolytic reaction via eq 1 at pH 5.5. The negligible difference in their yields could be explained by the higher bimolecular rate constant for $Cl^{\bullet}$ with HOCl (3.2×10^9 M^{-1} s^{-1}) compared with the bimolecular rate constant between $HO^{\bullet}$ and HOCl (2×10^9 M^{-1} s^{-1}). In NOM solutions, the formation of $HO^{\bullet}$ decreased upon increasing the NOM concentration in the range of 0−2.0 mg-C L^{-1}. In contrast, the formation of $Cl^{\bullet}$ increased upon increasing the NOM concentration in the range of 0−1.0 mg-C L^{-1}. Upon further increasing the NOM concentration to 2.0 mg-C L^{-1}, the increase rate slowed down. The influence of NOM on the total free radical yield was further investigated. As shown in Figure S2 of the Supporting Information, the total free radical yield increased upon increasing the NOM concentration in the range of 0−2.0 mg-C, which indicated the promoting effect of NOM on radical formation via the photolysis of FAC under simulated solar irradiation. Hence, the reaction mechanism involved the electron transfer from excited singlet phenolic compounds in NOM to FAC, which yielded $Cl^{\bullet}$ in the solar/chlorine system. Based on the above results, it can be speculated that NOM will accelerate the degradation of "chlorine radicals-controlled" micropollutant and inhibit the degradation of "hydroxyl radicals-controlled" micropollutant in the solar/chlorine system.

CONCLUSIONS

The solar/chlorine system has been proposed as a novel AOP that can efficiently abate refractory pollutants and disinfect by producing a suite of RS including $HO^{\bullet}$, $Cl^{\bullet}$, $ClO^{\bullet}$, O_3, and so forth. Just as with other AOPs, understanding the formation of RS is essential for future applications of the solar/chlorine system for water treatment or disinfection. The solar photolysis of FAC was dramatically accelerated in the presence of NOM due to the reaction between photoexcited NOM and FAC. Employing DO control experiments, EDC measurements, and a model phenolic compound, the reaction mechanism was elucidated. The influence of NOM on $HO^{\bullet}$ and $Cl^{\bullet}$ formation by the solar/chlorine system was measured in detail. Photoexcited NOM might play a significant role in accelerating the formation of $Cl^{\bullet}$ in the solar/chlorine system at pH 5.5. These data will be useful in predicting the removal of organic pollutants from wastewater when treated using the solar/chlorine process. Toxic chlorinated DBPs are usually generated from the reaction between chlorinated radicals such as $Cl^{\bullet}$ and $ClO^{\bullet}$ with NOM. The acceleration of $Cl^{\bullet}$ formation in the solar/chlorine system by photoexcited NOM should be taken into account when employing the solar/chlorine system for advanced oxidation. These findings can also help to explain some abnormal degradation behaviors in the previous literature. For example, the high degradation rates of several PPCPs (*N*,*N*-diethyl-3-methylbenzamide, caffeine, and carbamazepine) in the solar/chlorine system may have resulted from the formation of excess reactive $Cl^{\bullet}$ from the reaction between FAC and photoexcited PPCPs or NOMs, which further degraded PPCPs in subsequent reactions. In summary, this study provides a useful insight for the future applications of the solar/chlorine system as a novel AOP for wastewater treatment or disinfection.

ASSOCIATED CONTENT

Supporting Information

The Supporting Information is available free of charge at https://pubs.acs.org/doi/10.1021/acsomega.1c06616.

Extraction of EfOM; liquid system for the determination of EDC in various organic matters; EDC values in reference NOMs and EfOM; bimolecular reaction rate constants between RS and chemical probes; spectra for natural sunlight and the solar simulator and UV−vis spectra of FAC; and influence of the NOM concentration on the total radical yields (PDF)

AUTHOR INFORMATION

Corresponding Author

Dongxue Xiao − *Department of Environmental Science & Engineering, Fudan University, Shanghai 200433, P. R. China*; Phone: (+86)-21-3124-8921; Email: xiaoxue3300@163.com

Author

Huaxi Zhou − *Department of Environmental Science & Engineering, Fudan University, Shanghai 200433, P. R. China*; orcid.org/0000-0002-1592-982X

Complete contact information is available at: https://pubs.acs.org/10.1021/acsomega.1c06616

Notes

The authors declare no competing financial interest.

ACKNOWLEDGMENTS

We are thankful for funding support from the National Natural Science Foundation of China (21906025). H.Z. also appreciates the financial support from the China Postdoctoral Science Foundation (2019M651366).

REFERENCES

(1) Tsolaki, E.; Diamadopoulos, E. Technologies for ballast water treatment: a review. *J. Chem. Technol. Biotechnol.* **2010**, *85*, 19−32.

(2) Dias, R. P.; Schammel, M. H.; Reber, K. P.; Sivey, J. D. Applications of 1,3,5-trimethoxybenzene as a derivatizing agent for quantifying free chlorine, free bromine, bromamines, and bromide in aqueous systems. *Anal. Methods* **2019**, *11*, 5521−5532.

(3) Guo, K.; Wu, Z.; Shang, C.; Yao, B.; Hou, S.; Yang, X.; Song, W.; Fang, J. Radical chemistry and structural relationships of PPCP degradation by UV/chlorine treatment in simulated drinking water. *Environ. Sci. Technol.* **2017**, *51*, 10431−10439.

(4) Cheng, S.; Zhang, X.; Yang, X.; Shang, C.; Song, W.; Fang, J.; Pan, Y. The multiple role of bromide ion in PPCPs degradation under UV/chlorine treatment. *Environ. Sci. Technol.* **2018**, *52*, 1806−1816.

(5) Duan, X.; Sanan, T.; de la Cruz, A.; He, X.; Kong, M.; Dionysiou, D. D. Susceptibility of the algal toxin microcystin-LR to UV/chlorine process: Comparison with chlorination. *Environ. Sci. Technol.* **2018**, *52*, 8252−8262.

(6) Zhang, R.; Meng, T.; Huang, C.-H.; Ben, W.; Yao, H.; Liu, R.; Sun, P. PPCP degradation by chlorine-UV processes in ammoniacal water: New reaction insights, kinetic modeling, and DBP formation. *Environ. Sci. Technol.* **2018**, *52*, 7833−7841.

(7) Fang, J.; Fu, Y.; Shang, C. The roles of reactive species in micropollutant degradation in the UV/free chlorine system. *Environ. Sci. Technol.* **2014**, *48*, 1859−1868.

(8) Jin, J.; El-Din, M. G.; Bolton, J. R. Assessment of the UV/chlorine process as an advanced oxidation process. *Water Res.* **2011**, *45*, 1890−1896.

(9) Deng, L.; Huang, C.-H.; Wang, Y.-L. Effects of combined UV and chlorine treatment on the formation of trichloronitromethane from amine precursors. *Environ. Sci. Technol.* **2014**, *48*, 2697−2705.
(10) Chan, P. Y.; El-Din, M. G.; Bolton, J. R. A solar-driven UV/chlorine advanced oxidation process. *Water Res.* **2012**, *46*, 5672−5682.
(11) Forsyth, J. E.; Zhou, P.; Mao, Q.; Asato, S. S.; Meschke, J. S.; Dodd, M. C. Enhanced inactivation of bacillus subtilis spores during solar photolysis of free available chlorine. *Environ. Sci. Technol.* **2013**, *47*, 12976−12984.
(12) Shu, Z.; Li, C.; Belosevic, M.; Bolton, J. R.; El-Din, M. G. Application of a solar UV/chlorine advanced oxidation process to oil sands process-affected water remediation. *Environ. Sci. Technol.* **2014**, *48*, 9692−9701.
(13) Zhou, P.; Di Giovanni, G. D.; Meschke, J. S.; Dodd, M. C. Enhanced inactivation of cryptosporidium parvum oocysts during solar photolysis of free available chlorine. *Environ. Sci. Technol. Lett.* **2014**, *1*, 453−458.
(14) Sun, P.; Lee, W.-N.; Zhang, R.; Huang, C.-H. Degradation of DEET and caffeine under UV/chlorine and simulated sunlight/chlorine conditions. *Environ. Sci. Technol.* **2016**, *50*, 13265−13273.
(15) Yang, B.; Kookana, R. S.; Williams, M.; Du, J.; Doan, H.; Kumar, A. Removal of carbamazepine in aqueous solutions through solar photolysis of free available chlorine. *Water Res.* **2016**, *100*, 413−420.
(16) Young, T. R.; Li, W.; Guo, A.; Korshin, G. V.; Dodd, M. C. Characterization of disinfection byproduct formation and associated changes to dissolved organic matter during solar photolysis of free available chlorine. *Water Res.* **2018**, *146*, 318−327.
(17) Bulman, D. M.; Mezyk, S. P.; Remucal, C. K. The impact of pH and irradiation wavelength on the production of reactive oxidants during chlorine photolysis. *Environ. Sci. Technol.* **2019**, *53*, 4450−4459.
(18) Cheng, S.; Zhang, X.; Song, W.; Pan, Y.; Lambropoulou, D.; Zhong, Y.; Du, Y.; Nie, J.; Yang, X. Photochemical oxidation of PPCPs using a combination of solar irradiation and free available chlorine. *Sci. Total Environ.* **2019**, *682*, 629−638.
(19) Hua, Z.; Guo, K.; Kong, X.; Lin, S.; Wu, Z.; Wang, L.; Huang, H.; Fang, J. PPCP degradation and DBP formation in the solar/free chlorine system: Effects of pH and dissolved oxygen. *Water Res.* **2019**, *150*, 77−85.
(20) Sun, J. L.; Bu, L. J.; Chen, S. Y.; Lu, X. L.; Wu, Y. T.; Shi, Z.; Zhou, S. Q. Oxidation of Microcystic-LR via the solar/chlorine process: Radical mechanism, pathways and toxicity assessment. *Ecotoxicol. Environ. Saf.* **2019**, *183*, 7.
(21) Buxton, G. V.; Subhani, M. S. Radiation-chemistry and photochemistry of oxychlorine ions. part 2.-Photodecomposition of aqueous-solutions of hypochlorite ions. *J. Chem. Soc., Faraday Trans. 1* **1972**, *68*, 958.
(22) Molina, M. J.; Ishiwata, T.; Molina, L. T. Production of OH from photolysis of HOCI at 307-309 nm. *J. Phys. Chem.* **1980**, *84*, 821−826.
(23) Nowell, L. H.; Hoigné, J. Photolysis of aqueous chlorine at sunlight and ultraviolet wavelengths - 2. Hydroxyl radical production. *Water Res.* **1992**, *26*, 599−605.
(24) Leitzke, A.; Reisz, E.; Flyunt, R.; von Sonntag, C. The reactions of ozone with cinnamic acids: formation and decay of 2-hydroperoxy-2-hydroxyacetic acid. *J. Chem. Soc., Perkin Trans. 2* **2001**, 793−797.
(25) Alfassi, Z. B.; Huie, R. E.; Mosseri, S.; Neta, P. Kinetics of one-electron oxidation by the ClO radical. *Radiat. Phys. Chem.* **1988**, *32*, 85−88.
(26) Hasegawa, K.; Neta, P. Rate constants and mechanisms of reaction of $Cl_2^{\bullet-}$ radicals. *J. Phys. Chem.* **1978**, *82*, 854−857.
(27) Kong, X. J.; Wang, L. P.; Wu, Z. H.; Zeng, F. L.; Sun, H. Y.; Guo, K. H.; Hua, Z. C.; Fang, J. Y. Solar irradiation combined with chlorine can detoxify herbicides. *Water Res.* **2020**, *177*, 11.
(28) Coble, P. G. Characterization of marine and terrestrial DOM in seawater using excitation-emission matrix spectroscopy. *Mar. Chem.* **1996**, *51*, 325−346.
(29) Leenheer, J. A.; Croué, J.-P.; Benjamin, M.; Korshin, G. V.; Hwang, C. J.; Bruchet, A.; Aiken, G. R., Comprehensive isolation of natural organic matter from water for spectral characterizations and reactivity testing. *Natural Organic Matter and Disinfection By-Products*; American Chemical Society, 2000; Vol. *761*, pp 68−83.
(30) Gonsior, M.; Peake, B. M.; Cooper, W. T.; Podgorski, D.; D'Andrilli, J.; Cooper, W. J. Photochemically induced changes in dissolved organic matter identified by ultrahigh resolution fourier transform ion cyclotron resonance mass spectrometry. *Environ. Sci. Technol.* **2009**, *43*, 698−703.
(31) Zhang, D.; Yan, S.; Song, W. Photochemically induced formation of reactive oxygen species (ROS) from effluent organic matter. *Environ. Sci. Technol.* **2014**, *48*, 12645−12653.
(32) Maizel, A. C.; Remucal, C. K. Molecular composition and photochemical reactivity of size-fractionated dissolved organic matter. *Environ. Sci. Technol.* **2017**, *51*, 2113−2123.
(33) Jaffé, R.; Yamashita, Y.; Maie, N.; Cooper, W. T.; Dittmar, T.; Dodds, W. K.; Jones, J. B.; Myoshi, T.; Ortiz-Zayas, J. R.; Podgorski, D. C.; Watanabe, A. Dissolved organic matter in headwater streams: Compositional variability across climatic regions of North America. *Geochim. Cosmochim. Acta* **2012**, *94*, 95−108.
(34) Zepp, R. G.; Schlotzhauer, P. F.; Sink, R. M. Photosensitized transformations involving electronic energy transfer in natural waters: Role of humic substances. *Environ. Sci. Technol.* **1985**, *19*, 74−81.
(35) McNeill, K.; Canonica, S. Triplet state dissolved organic matter in aquatic photochemistry: reaction mechanisms, substrate scope, and photophysical properties. *Environ. Sci.: Processes Impacts* **2016**, *18*, 1381−1399.
(36) Lambert, C. R.; Kochevar, I. E. Electron transfer quenching of the rose bengal triplet state. *Photochem. Photobiol.* **1997**, *66*, 15−25.
(37) Koppenol, W. H.; Stanbury, D. M.; Bounds, P. L. Electrode potentials of partially reduced oxygen species, from dioxygen to water. *Free Radical Biol. Med.* **2010**, *49*, 317−322.
(38) Bond, T.; Henriet, O.; Goslan, E. H.; Parsons, S. A.; Jefferson, B. Disinfection byproduct formation and fractionation behavior of natural organic matter surrogates. *Environ. Sci. Technol.* **2009**, *43*, 5982−5989.
(39) Kanan, A.; Karanfil, T. Formation of disinfection by-products in indoor swimming pool water: The contribution from filling water natural organic matter and swimmer body fluids. *Water Res.* **2011**, *45*, 926−932.
(40) Bodhipaksha, L. C.; Sharpless, C. M.; Chin, Y.-P.; Sander, M.; Langston, W. K.; Mackay, A. A. Triplet photochemistry of effluent and natural organic matter in whole water and isolates from effluent-receiving rivers. *Environ. Sci. Technol.* **2015**, *49*, 3453−3463.
(41) Zhou, H.; Yan, S.; Lian, L.; Song, W. Triplet-state photochemistry of dissolved organic matter: Triplet-state energy distribution and surface electric charge conditions. *Environ. Sci. Technol.* **2019**, *53*, 2482−2490.
(42) Moore, H. E.; Garmendia, M. J.; Cooper, W. J. Kinetics of monochloramine oxidation of N,N-diethyl-p-phenylenediamine. *Environ. Sci. Technol.* **1984**, *18*, 348−353.
(43) Zhou, H.; Yan, S.; Ma, J.; Lian, L.; Song, W. Development of novel chemical probes for examining triplet natural organic matter under solar illumination. *Environ. Sci. Technol.* **2017**, *51*, 11066−11074.
(44) Önnby, L.; Walpen, N.; Salhi, E.; Sander, M.; von Gunten, U. Two analytical approaches quantifying the electron donating capacities of dissolved organic matter to monitor its oxidation during chlorination and ozonation. *Water Res.* **2018**, *144*, 677−689.
(45) Janssen, E. M.-L.; Erickson, P. R.; McNeill, K. Dual roles of dissolved organic matter as sensitizer and quencher in the photooxidation of tryptophan. *Environ. Sci. Technol.* **2014**, *48*, 4916−4924.
(46) Wenk, J.; Aeschbacher, M.; Sander, M.; Gunten, U. V.; Canonica, S. Photosensitizing and inhibitory effects of ozonated dissolved organic matter on triplet-induced contaminant transformation. *Environ. Sci. Technol.* **2015**, *49*, 8541−8549.

https://doi.org/10.1021/acsomega.1c06616
ACS Omega 2022, 7, 7769−7776

(47) Wenk, J.; Canonica, S. Phenolic antioxidants inhibit the triplet-induced transformation of anilines and sulfonamide antibiotics in aqueous solution. *Environ. Sci. Technol.* **2012**, *46*, 5455−5462.
(48) Page, S. E.; Logan, J. R.; Cory, R. M.; McNeill, K. Evidence for dissolved organic matter as the primary source and sink of photochemically produced hydroxyl radical in arctic surface waters. *Environ. Sci.: Processes Impacts* **2014**, *16*, 807−822.
(49) Latch, D. E.; McNeill, K. Microheterogeneity of singlet oxygen distributions in irradiated humic acid solutions. *Science* **2006**, *311*, 1743−1747.
(50) Zhang, Y.; Blough, N. V. Photoproduction of one-electron reducing intermediates by chromophoric dissolved organic matter (CDOM): Relation to $O_2^{\cdot-}$ and H_2O_2 photoproduction and CDOM photooxidation. *Environ. Sci. Technol.* **2016**, *50*, 11008−11015.
(51) Garg, S.; Rose, A. L.; Waite, T. D. Superoxide mediated reduction of organically complexed Iron(III): Comparison of non-dissociative and dissociative reduction pathways. *Environ. Sci. Technol.* **2007**, *41*, 3205−3212.
(52) Pham, A. N.; Xing, G.; Miller, C. J.; Waite, T. D. Fenton-like copper redox chemistry revisited: Hydrogen peroxide and superoxide mediation of copper-catalyzed oxidant production. *J. Catal.* **2013**, *301*, 54−64.
(53) Aeschbacher, M.; Graf, C.; Schwarzenbach, R. P.; Sander, M. Antioxidant properties of humic substances. *Environ. Sci. Technol.* **2012**, *46*, 4916−4925.
(54) Aeschbacher, M.; Sander, M.; Schwarzenbach, R. P. Novel electrochemical approach to assess the redox properties of humic substances. *Environ. Sci. Technol.* **2010**, *44*, 87−93.
(55) Önnby, L.; Salhi, E.; McKay, G.; Rosario-Ortiz, F. L.; von Gunten, U. Ozone and chlorine reactions with dissolved organic matter - Assessment of oxidant-reactive moieties by optical measurements and the electron donating capacities. *Water Res.* **2018**, *144*, 64−75.
(56) Zhou, H.; Lian, L.; Yan, S.; Song, W. Insights into the photo-induced formation of reactive intermediates from effluent organic matter: The role of chemical constituents. *Water Res.* **2017**, *112*, 120−128.
(57) Bahnmüller, S.; von Gunten, U.; Canonica, S. Sunlight-induced transformation of sulfadiazine and sulfamethoxazole in surface waters and wastewater effluents. *Water Res.* **2014**, *57*, 183−192.
(58) Guerard, J. J.; Chin, Y.-P.; Mash, H.; Hadad, C. M. Photochemical fate of sulfadimethoxine in aquaculture waters. *Environ. Sci. Technol.* **2009**, *43*, 8587−8592.
(59) Canonica, S.; Jans, U.; Stemmler, K.; Hoigne, J. Transformation kinetics of phenols in water: Photosensitization by dissolved natural organic material and aromatic ketones. *Environ. Sci. Technol.* **1995**, *29*, 1822−1831.
(60) Buxton, G. V.; Greenstock, C. L.; Helman, W. P.; Ross, A. B. Critical review of rate constants for reactions of hydrated electrons, hydrogen-atoms and hydroxyl radicals ($\bullet OH/\bullet O^-$) in aqueous solution. *J. Phys. Chem. Ref. Data* **1988**, *17*, 513−886.
(61) Mártire, D. O.; Rosso, J. A.; Bertolotti, S.; Le Roux, G. C.; Braun, A. M.; Gonzalez, M. C. Kinetic study of the reactions of chlorine atoms and $Cl_2^{\bullet-}$ radical anions in aqueous solutions. II. Toluene, benzoic acid, and chlorobenzene. *J. Phys. Chem. A* **2001**, *105*, 5385−5392.

https://doi.org/10.1021/acsomega.1c06616
ACS Omega 2022, 7, 7769−7776